SCIENCE CHINA
Information Sciences

• RESEARCH PAPER •
Special Focus on Robot Sensing and Dexterous Operation

December 2014, Vol. 57 120207:1–120207:11
doi: 10.1007/s11432-014-5216-3

In-hand haptic perception in dexterous manipulations

HE JunHu* & ZHANG JianWei*

Faculty of Mathematics, Informatics and Natural Sciences, Department Informatics, University of Hamburg, Hamburg 22527*, Germany*

Received July 12, 2014; accepted September 24, 2014; published online October 29, 2014

Abstract Dexterous in-hand manipulation with multi-finger robotic hands is a hot topic in robotics. Recently many famous multi-finger robotic hands have been developed. Though a lot of research has been done on them; in-hand manipulation is still a challenge. One of its issues lies in the uncertainty of interaction states. In this paper we research robot-object interaction from a novel angle called haptic exploration. This method helps robots acquire the ability to explore the robot-object interaction. In in-hand manipulation tasks, haptic exploration is a process where the robot pushes on in-hand objects slightly in different directions, and meanwhile perceives the haptic feedback to estimate the interaction state. In this paper a new single finger push model is proposed for analyzing the haptic feedback, which is similar to traditional impedance control of robot arm. In this model the stiffness of fingers, the deformation on contact surface, and the change of object's pos (position and attitude) are considered. Furthermore, a push resistance is given to describe the haptic feedback acquired from a slight push. Finally, real robotic experiments are conducted to verify the feasibility of proposed method.

Keywords in-hand manipulation, multi-finger robotic hands, dexterous manipulation, haptic perception, haptic feedback

Citation He J H, Zhang J W. In-hand haptic perception in dexterous manipulations. Sci China Inf Sci, 2014, 57: 120207(11), doi: 10.1007/s11432-014-5216-3

1 Introduction

Dexterous manipulation with multi-fingered robot hands are gaining increasing attention for its potential applications. Recently, several famous anthropomorphic robotic hands have been developed, such as Shadow hand [1], Robonaut hand [2] and DLR/HIT hand [3] etc. One of their well-known essential anthroposophic skills is dexterous in-hand manipulation. The generally accepted conception of dexterous in-hand manipulation is a capability of changing the position and orientation of the manipulated objects from an initial configuration to a given one within one hand [4]. It enables the robotic hand not only to hold objects with a firm grasp, but also to move and position objects with fingers's actions.

The early robot hand research can be tracked back more then 30 years ago [5]. Lots of research have been done in the past decades in this field [4,6,7]; however most of them are still far away from real applications. Some dexterous manipulating tasks are still difficult to be carried out reliably even in laboratory environment. One of the issues lies in the uncertainty of robot-object interaction states; in

* Corresponding author (email: he@informatik.uni-hamburg.de, zhang@informatik.uni-hamburg.de)

other words, there are still a lack of effective approaches that describe the interaction state between the robot hand and objects.

In traditional robot hand control systems, when robots are controlled to manipulate grasp and regrasp objects, they should have complete knowledge about robot mechanics, target objects (geometry and physic proprieties, location in environment), and physical laws relating to interaction [8]. Therefore, in order to achieve a dexterous and skillful manipulation, the most intuitive methods are synthesize operations. One of these most impressive results is the high-speed manipulation [9–11]. It analyzed the robot-object interaction model to achieve the dynamic fast manipulations. In [12], Garcia and Parra built a dynamic model precisely to roll a rigid dynamic circular object with a hemispherical deformable fingertip. However synthetic operations are very labor intensive, and sometimes it is even impractical to build a precise robot-object interaction model.

Instead of building precise interaction models, some other researchers solved these issues with artificial intelligence methods [13,14]. Schaedle and Ertel [15] implemented hierarchal reinforcement learning to solve the problems associated with a high dimensional manipulation task. Both in grasping and in-hand manipulation, planning under contact conditions is usually impractical due to computational complexity and the lack of precise dynamics models. Hence some researches let robots learn to deal with these uncertainty problems. Kalakrishnan et al. [16] made their robot learn the force/torque compliance controller with Path Integral algorithm ($\mathbf{PI}^2$). In [17,18], authors employed reinforcement learning to help robots learn grasp skills. Gorce et al. [19] applied neural networks to deal with the insufficient knowledge problems. In [20], several learning schemes have been proposed for dexterous hand grasping and manipulation.

While some of these strategies can be used to improve the quality of interaction perception, the intelligent robotic system still requires better perception methods for skillful tasks. Therefore, in this paper a novel perception strategy called 'haptic exploration' is proposed to address the uncertainty interaction perception problems; here haptic exploration helps the robot to better perceive the interaction state with force feedback.

This paper is organized as follows: In Section 2, related works and research problems are discussed. In Section 3, the research conception is discussed and haptic push models are proposed. Then in Section 4, a dexterous in-hand manipulation system is introduced. Finally, in Section 5 a haptic exploration experiment is carried out and its results show the feasibility of the proposed haptic exploration method.

2 Problem definition and related works

Psychological research on human touch has revealed that force can overcome object geometry cues in the perception of shape during active touch [21], therefore this research is to perceive interaction from force cues. In this paper the push perception concerns more about the contact force (contact pressure from the sensors).

The term haptic exploration is very similar to 'touch exploration' and 'active touch' which are widely used in robot recognition fields. In 1990, Kenneth used active touch to explore and recognize a 3D object taken from a known set of models [22,23]. In [24,25], a real textured surface was detected with the active touch of a rigid probe.

However most touch exploration research focus on the static object information (liking geometry surface, texture etc.); very few of them pay attention on dynamic information during the interaction process. Thus the method 'haptic exploration' is introduced to illustrate a dynamic interaction state during an exploration process. For robotic dexterous manipulation, the haptic exploration is a process where the robot controls its fingers to push objects slightly in different given directions, and perceives the interaction state through its push feedback. Differently from pushing a box on the ground, in this paper the purpose of slight pushes is to perceive the resistance force information instead of moving objects. Therefore all the push presented in this paper is limited to a very small range. Further, the push feedback refers to the information collected by sensors, such as object deformation, joints' conditions, contact pressure and so on. In the experiments, the contact pressure is adopted as the feedback.

In earlier object force push interaction research, like [26], for 2D object push problems, precise analytical models were developed to plan push actions. For dexterous object-robot interaction research, most current researchers explore the interaction from modeling objects and robots separately, and combine the two with physical laws [9,27]. In contrast, the conception proposed in this work treats the target objects and their support as one black box system. In this paper, the support finger is the finger which is stationary during manipulation. With the conception of trial and error, haptic exploration can be a general method to help the robot collect enough knowledge for its interaction tasks. More importantly it makes the robot system escape from complicated physical laws and describes the interaction state with its push feedback directly.

3 Manipulation model

In order to simplify research problems, the following assumptions are considered:

(1) All robot actions are in workspace.
(2) The manipulating processes are quasi-static.
(3) The fingers and object are keep in contact.
(4) Every contact finger has only one contact point, which is located at the center of fingertip.
(5) The torque of joints is sufficient for all its push actions.

3.1 Equilibrium point control model for impedance

According to the equilibrium trajectory hypothesis, multi-joint arm movements are achieved by gradually shifting the hand's equilibrium positions defined by the neuromuscular [28,29]. In robotics, impedance control is a widely adopted method for robot contact tasks. And the impedance control law can be described as [30] (ignore the term $G(q)$):

$$\tau = \boldsymbol{J}^{\mathrm{T}}(q)(-\boldsymbol{K}_c(x - x_d) - \boldsymbol{B}_c\dot{x}), \tag{1}$$

where the vector x and $\dot{x}$ denote current position and velocity of end-effector respectively. The x_d is the desired position of end-effector. And the matrices $\boldsymbol{K}_c$ and $\boldsymbol{B}_c$ are stiffness and damping matrices in Cartesian space. The τ is the joints' torque generated by actuators. And the matrix $\boldsymbol{J}$ refers to Jacobin matrix. All the manipulation processes are quasi-static, hence the damping matrix $\boldsymbol{B}_c$ is $\mathbf{0}$.

As introduced in [28,31,32], this impedance control can be considered as an equilibrium point control. And hence the end-effector's stiffness matrix can be represented graphically as an ellipse, which can be described with 3 parameters $(\lambda_1, \lambda_2, \theta)$. As shown in Figure 1.

3.2 Push stiffness model

Generally, in an unknown environment it is hard to acquire the objects' external stiffness. However in robotic dexterous in-hand manipulation tasks, the object is supported by robotic fingers. Fortunately, this makes it easier to analyze the push stiffness. As a result, a single finger push stiffness model to estimate the stiffness of an object in Catesian space during robot-object interaction is proposed in this section.

The push stiffness model is shown in Figure 2. An object is grasped by two independent fingers. The upper finger is a push finger which is actuated to push in a vector S_p described with an angle θ; and the down fingers are support fingers which are slave (uncontrolled) and have compliance properties. Both the contact areas between fingers and the object are simplified as two fixed points: push point P and support point O_s. During push actions, the object rolls on the supported finger; and it rolls over an angle of γ. In this research we assume the rolling center is located at the contact point O_s.

Therefore, after a slight push, the position of the push point changes along the vector S_p. As shown in Figure 2, the back vector S_p is decomposed orthogonally into S_{pt} and S_{pn}. $S_{\mathrm{pt}} = S_p\cos(\theta)$, $S_{\mathrm{pn}} = S_p\sin(\theta)$. This movement S_p of push point P consists mainly of three parts: deformation in contact

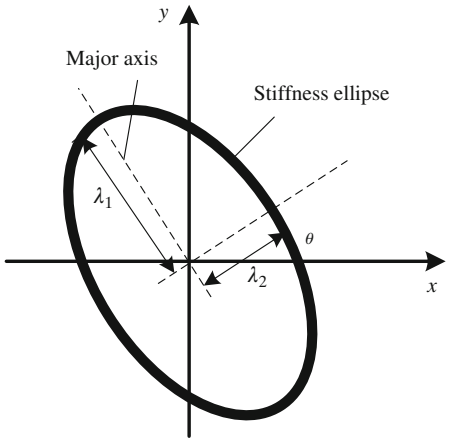

Figure 1 Graphical stiffness ellipse in Cartesian space. The parameters λ_1, λ_2 represent the length of major axis and minor axis respectively. And the angle θ denotes the orientation of the ellipse.

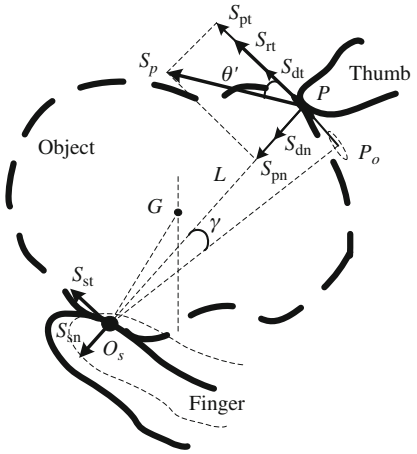

Figure 2 Single finger push.

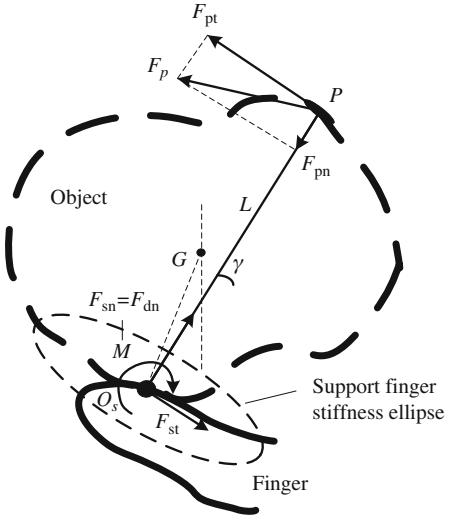

Figure 3 Push stiffness mode in dexterous manipulation tasks.

surface, object's rolling on the support finger, and compliance of the support finger. Hence the terms $S_{\rm pt}$ and $S_{\rm pn}$ can be expressed as:

$$S_{\rm pt} = S_{\rm st} + S_{\rm dt} + S_{\rm rt}, \tag{2}$$

$$S_{\rm pn} = S_{\rm sn} + S_{\rm dn}, \tag{3}$$

where the vectors $S_{\rm st}$, $S_{\rm sn}$ denote the change of the support finger's position along orthogonal directions; the vectors $S_{\rm dt}$, $S_{\rm dn}$ refer to the change of the push point's position for the deformation on contact surface; and the term $S_{\rm rt}$ is the change of the push point's position for object's rolling on the support finger. Obviously, compared to the rolling term $S_{\rm rt}$, the term $S_{\rm dt}$ from deformation is considered to be much smaller. Hence we assume $S_{\rm dt} = 0$.

3.3 Dexterous manipulation model

After a finger push, the change in push force is gained from the system's deformation. The force state is shown in Figure 3. Also the push force is orthogonally decomposed into two components $F_{\rm pn}$, $F_{\rm pt}$. And according to the equilibrium conditions, the push force can be expressed as:

$$F_{\rm pt} = F_{\rm st} = F_{\rm dt} = T/L, \tag{4}$$

$$F_{\rm pn} = F_{\rm sn} = F_{\rm dn}, \tag{5}$$

where the terms $F_{\rm dt}$, $F_{\rm dn}$ are deformation forces which causes the deformation on object-fingers contact surface; the terms $F_{\rm st}$, $F_{\rm sn}$ denote the compliance force produced by the support finger; the term T, L refer to the rolling torque and the length between two contact points P, O_s respectively. For the complexity of elastic objects, the relationship between the deformation on contact surface and contact force is very complex. It relates to many factors such as material of object and surface, shape of contact area, contact force applied on object etc. [33]. In this paper, these are just simplified to be $F_{\rm dn} = K_{\rm dn}S_{\rm dn}$, where the $K_{\rm dn}$ is a special elasticity coefficient.

As introduced in Subsection 3.1, the stiffness ellipse model is adopted to describe compliance stiffness on the support finger. $F_{\rm st} = K_{\rm st}S_{\rm st}$, $F_{\rm sn} = K_{\rm sn}S_{\rm sn}$. And the term $K_{\rm sn}$, $K_{\rm st}$ are the stiffness acquired from the stiffness ellipse model.

Therefore the normal component of push force $F_{\rm pn}$ can be expressed with $P_{\rm pn}$:

$$F_{\rm pn} = \frac{K_{\rm sn}K_{\rm dn}}{K_{\rm sn} + K_{\rm dn}} S_p \sin(\theta). \tag{6}$$

3.4 Two rolling cases

Two cases are under consideration depending on whether the object is rolled or unrolled during the thumb push actions.

3.4.1 *Rolled case*

The rolled case is when the object rolls on the support finger. In this case, since the object rolls on the finger, the displacement $S_{\rm rt}$ is much larger than the term $S_{\rm dt}$ which is produced by deformation. Hence in this case we assume $S_{\rm dt} = 0$ and the toque T is rolling friction which can be calculated from:

$$T = C_{\rm rr}F_{\rm pn}L, \tag{7}$$

where the $C_{\rm rr}$ is the rolling friction coefficient. Therefore, from the (4), (6), (7) the tangential component of push force $F_{\rm pt}$ can be expressed with P_p:

$$F_{\rm pt} = \frac{K_{\rm sn}K_{\rm dn}}{K_{\rm sn} + K_{\rm dn}} C_{\rm rr} S_p \sin(\theta). \tag{8}$$

3.4.2 *Unrolled case*

On the other hand, in the unrolled case the object does not roll on the support finger. In this case, the rolling torque T is produced from the surface deformation. Here the relation between rolling torque and deformed angle γ is simplified with a linear model:

$$T = C_d\gamma, \tag{9}$$

where the C_d refers to the linear coefficient for deformation. Therefore from (2), (9), the tangential component of push force $F_{\rm pt}$ can be expressed with P_p:

$$F_{\rm pt} = \frac{K_{\rm st}C_d}{L^2K_{\rm st} + C_d} S_p \cos(\theta). \tag{10}$$

3.4.3 *Critical conditions*

The critical condition between these two cases is (8) = (10); that is

$$\theta_c = \arctan \frac{1}{K_{\rm dn}} \frac{K_{\rm st}}{K_{\rm sn}} \frac{C_d}{C_{\rm rr}} \frac{K_{\rm sn} + K_{\rm dn}}{L^2K_{\rm st} + C_d}. \tag{11}$$

It is worth noting that, actually, the θ_c is not a precise angle value. For reason that in the rolling case, both deformation and rolling exist. Thus the shift between these two cases can be more continuous and smooth.

Figure 4 Shadow hand.

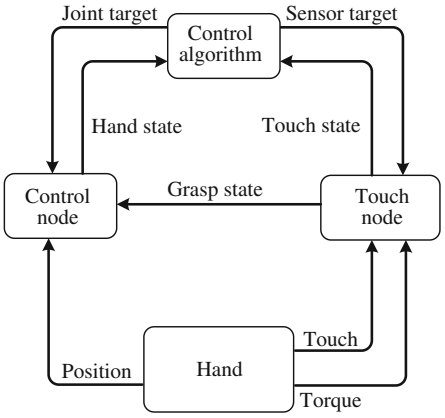

Figure 5 Software system.

3.5 Push resistance

Similar to impedance, the push resistance is introduced in this section. The push resistance is used to measure the impedance state and its practical effect while a finger pushes in a specific direction. Hence a simple way to express the push resistance P_r is:

$$P_r = \frac{F_p}{S_p}. \tag{12}$$

With limited accuracy of our robot hand, it is impossible to change the term S_p with different small values. Thus in this paper we just assume that the term S_p is a constant.

For the rolled case the push resistance $P_{\rm rr}$ is:

$$P_{\rm rr} = \frac{K_{\rm sn}K_{\rm dn}}{K_{\rm sn}+K_{\rm dn}}|C_{\rm rr}\sin(\theta)\boldsymbol{i} + \sin(\theta)\boldsymbol{j}|, \tag{13}$$

where the $\boldsymbol{i}$, $\boldsymbol{j}$ denote the unit vectors of axes $\boldsymbol{x}$, $\boldsymbol{y}$ respectively. And for the rolled case the push resistance $P_{\rm ru}$ is:

$$P_{\rm ru} = \left|\frac{K_{\rm st}C_r}{L^2K_{\rm st}+C_r}\cos(\theta)\boldsymbol{i} + \frac{K_{\rm sn}K_{\rm dn}}{K_{\rm sn}+K_{\rm dn}}\sin(\theta)\boldsymbol{j}\right|. \tag{14}$$

Although there are many parameters used to describe the robot push force, many of them mainly relate to the robot itself. Therefore, it is more practical to estimate these parameters before manipulation tasks.

4 Dexterous manipulation system

A multi-fingered robotic hand system is built for dexterous manipulation. Generally, it can be divided into two parts: hardware and software.

4.1 Hardware

In Figure 4 the multi-fingered hand and sensors are shown. In this system the robot hand is shadow hand[1)]. It takes a truly anthropomorphic approach to robot manipulation, totaling 20 degrees of freedom. The tactile sensors mounted on this hand are BioTac[2)], which have the force, vibration and temperature sensing capabilities by mimicking human fingertips. In this paper the direct pressure is adopted to estimate the push force between fingertips and the object.

1) Shadow dexterous hand: http://www.shadowrobot.com.
2) Biotac: http://www.syntouchllc.com/.

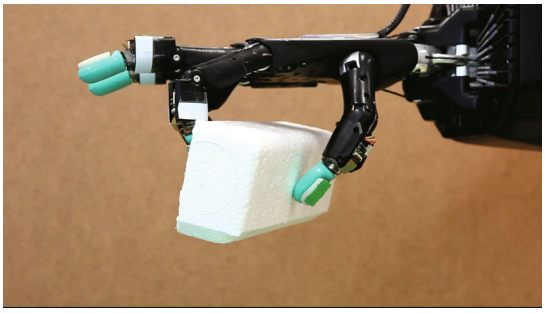

Figure 6 In-hand manipulation experiment.

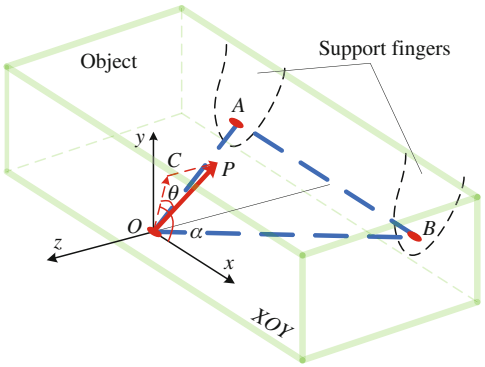

Figure 7 Three fingers' grasping frame.

4.2 Software

A specifical robot control software is developed under ROS[3]. The software architecture is shown in Figure 5. In this system there are three main nodes: algorithm node, position node, and touch node. The algorithm node is to plan the actions of robotic fingers. The control node is for executing the finger actions. And the touch node collects all the fingertip tactile sensation, joints' torque and position information and does some preliminary data processing.

5 Experiments

In order to verify the manipulation method and model, the push manipulation experiments were conducted on a real shadow hand. The task of these experiments was making the thumb push a cubic object in different directions, and observing the tactile feedback. With the observed tactile data, the spatial push resistance can be estimated, which can be used in robotic dexterous manipulation control. The object used in these experiments is a foam rectangle box with the dimension of 160 mm × 70 mm × 40 mm, as shown in Figure 6. We chose it for three reasons. First, in these push experiments, the object should be neither too hard nor too soft for protecting our robot hand. Second as described in Subsection 3.4, the contact surface is the flatter the better to meet the rolling case. At last, in the proposed model the gravity is ignored, thus the object should be light.

In the push stiffness model section, only two fingers are discussed but in these experiments the three fingers' grasp is adopted. There are two reasons. One reason is that the three fingers grasp is more stable than that of two. It ensures the reproducibility of the experiments. The other reason is that the two fingers' grasping does not easily reflect the advantage of haptic exploration. Three fingers' grasp makes the push resistance different with the different parameter α in Figure 7, and its result is as shown in Figure 8.

5.1 Object push directions

In Figure 7, a cubic object is grasped by 3 fingers. The 3 red dots refer to the 3 contact points (A,B,O) located on the surface of the object. The two fingers behind the box are support fingers which are fixed without any active movement during the push manipulations. The finger in front of the object is the push finger, which can be controlled actively to push objects in given directions. A push frame is fixed on the push contact point O with its origin located at the point O. Its axis x is parallel to the support contact line AB; its axis y is perpendicular to the plane ABO. The red vector $\boldsymbol{OP}$ denotes a specifical push vector. Therefore, the thumb push vector $\boldsymbol{OP}$ can be described with three parameters: θ, α, and d. The parameter θ refers to the angle between the push vector $\boldsymbol{OP}$ and the plane XOY; the parameter α refers to the angle between axis x and the projected vector $\boldsymbol{OC}$ which is the projected vector of $\boldsymbol{OP}$ in

3) Ros: http://wiki.ros.org.

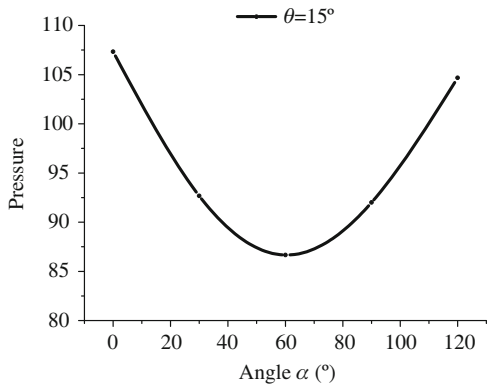

Figure 8 The push results when the thumb pushes in different angle $\alpha = 0^\circ$ to 120° with the angle $\theta = 15^\circ$.

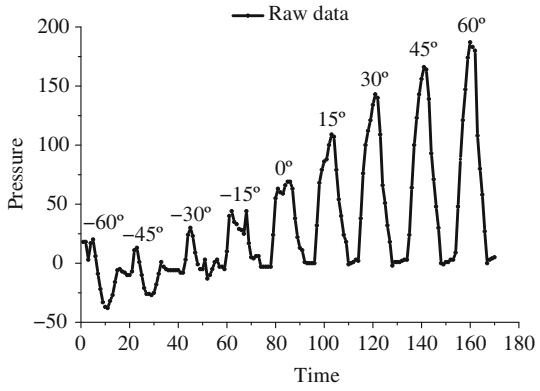

Figure 9 Raw data of push feedback, where the the angle $\alpha = 90^\circ$ and the thumb pushes in different directions with the angle $\theta = -60^\circ$ to 60°.

plane XOY; and the parameter d refers to the length of push vector $\boldsymbol{OP}$. In this experiment, the push actions are conducted in two steps, first forward push and then backwards push. In the forward push process, the push finger pushes along the vector $\boldsymbol{OP}$. In the backwards push process, the push finger moves back to origin O along the forward push trajectory.

One thing worth mentioning is that all these push actions are controlled off-line and the resolution of each joint is 1°. Because of such joints' resolutions, in these experiments, we set the length of push vector $\boldsymbol{OP}$ as a constant 5 mm ($d = 5$ mm). Therefore, the push resistance is the pressure value which can be collected from the tactile sensors directly.

Though the low level controller on shadow hand is PID control, the push actions are still limited by robotic structure. However with the conception of haptic exploration, both the limitation from the push finger's structure and the control resolution are part of the environment for this perceiving agent.

5.2 Data processing and experiment results

In this paper, the experiments were carried out in two parts. Firstly, the angle α was fixed and the thumb was controlled to push with different angle θ. Secondly, the angle θ was fixed and the thumb was controlled to push with different angle α.

5.2.1 *Push with fixed α*

The collected raw data in first segment is shown in Figure 9, where the blue line denotes the push feedback collected from syntouh sensor which is mounted on the tip of thumb. In addition the vertical and horizonal axes refer to the experiment time and the push pressure value respectively. Thus the peaks were produced by the push of the thumb. With different push directions, different peaks are acquired. While the angle α is fixed, $\alpha = 90^\circ$, the peaks from left to right relate to different value of angle θ, with $\theta = -60^\circ$, -45°, -30°, -15°, 0°, 15°, 30°, 45°, 60°.

In this paper we focus on the height of each peak. The height of each peak is calculated from the value of its highest point (at the middle point for each push) minus the value of its lowest point (at initial point for each push). Besides, in this experiment for each direction, each push actions is carried out 3 times. We calculated the average of them and plot it in Figure 10. In Figure 10 different color lines denote the push results with different fixed angle α. From the Figure 10, the relationship between push angle θ and push feedback can be considered as a linear model.

5.2.2 *Push with fixed θ*

The collected raw data in the second segment is shown in Figure 11, where the blue line also denotes the push feedback collected from syntouh sensor with a fixed angle $\theta = 15^\circ$. Similarly to Figure 9, the

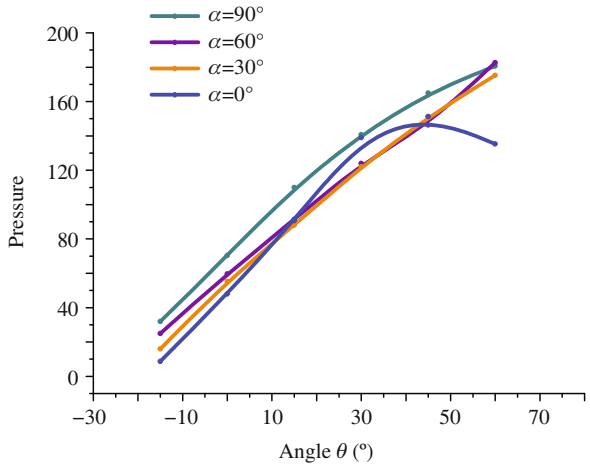

Figure 10 The push results when the thumb pushes in different angles $\theta = -60°$ *to* $60°$ with the angle $\theta = -15°$. In this figure, the different lines refer to different fixed angle $\alpha = 90°, 60°, 30°, 0°$.

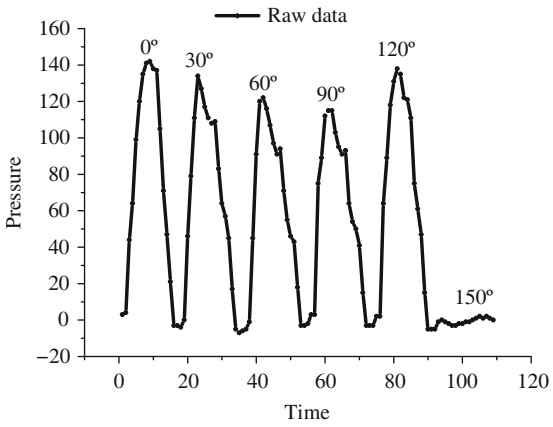

Figure 11 Raw data of push feedback, where the the angle $\theta = 15°$ and the thumb pushes in different directions with the angle $\alpha = 0°$ to $150°$.

vertical and horizonal axes refer to the time and the push pressure respectively. Therefore each peak denotes one push. While the angle θ is fixed to 15°, the peaks from left to right relate to different α values, with $\theta = 0°$, 30°, 60°, 90°, 120°, 150°. It is worth noting that θ never equals to 180°. This is because under the current grasp configuration, the push direction with $\theta = 180°$ can not be reached. In other words, this direction is out of the finger's workspace.

Also the height of peaks are considered in this part of experiment; and each action is also carried out 3 times along given directions. The average value of peaks' height is plotted in Figure 8. From this figure, a significant concave curve is shown.

If we define the best push direction α^* as a direction with smallest push resistance (feedback). From this view, this best push direction can be estimated from the Figure 8, it is located at around 65° (lowest point). Though theoretically the best push direction should be at the position $\alpha^* = 90°$; the deformation of contact surface, error relating to contact position, the compliance propriety of robot fingers and the accuracy of robot control system, all these affect best push direction in the manipulation tasks. Though most of them are hard to be estimated; with this haptic exploration method the best push direction can be found out directly from the smallest push resistance point.

6 Conclusion and future work

This paper gives a new insight to the perception of robot-object interaction in multi-finger dexterous manipulations. We make the robot system perceive the robot-object interaction state from trail and error. In order to evaluate the push feedback, push resistance has been proposed in this paper. Further, a synthetic push stiffness model is given to interpret the principle of push resistance in this paper. At last real robotic experiments have been carried out. In these experiments, the robot is controlled to push in given directions, which perceives the pressure feedback. With the feedback, the interaction state can be estimated, to find out the best push direction. Finally, the results of the experiments show the feasibility of our proposed method.

In the future, there are still lots of work to be done. On one hand, more experiments with different objects and different grasp configurations should be conducted. On the other hand, besides haptic feedback, other modalities (like vision) should be employed into this system for a better manipulation performance.

Acknowledgements

This research was supported by CINACS DFG IGK 1247, Robot-ERA FP7 CP 288899, and RACE FP7-ICT-2011-7 287752.

References

1 Kochan A. Shadow delivers first hand. Indl robot, 2005, 32: 15–16
2 Lovchik C, Diftler M A. The robonaut hand: a dexterous robot hand for space. In: Proceedings of the IEEE International Conference on Robotics and Automation (ICRA), Detroit, 1999. 907–912
3 Butterfass J, Grebenstein M, Liu H, et al. Dlr-hand ii: next generation of a dextrous robot hand. In: Proceedings of the IEEE International Conference on Robotics and Automation (ICRA), Seoul, 2001. 109–114
4 Bicchi A. Hands for dexterous manipulation and robust grasping: a difficult road toward simplicity. IEEE Trans Robotics Automat, 2000, 16: 652–662
5 Bicchi A, Kumar V. Robotic grasping and contact: a review. In: Proceedings of the IEEE International Conference on Robotics and Automation (ICRA), San Francisco, 2000. 348–353
6 Himoga K B. Robot grasp synthesis algorithms: a survey. Int J Robot Res, 1996, 15: 230–266
7 Okamura A M, Smaby N, Cutkosky M R. An overview of dexterous manipulation. In: Proceedings of the IEEE International Conference on Robotics and Automation (ICRA), San Francisco, 2000. 255–262
8 Khalil F F, Payeur P. Dexterous robotic manipulation of deformable objects with multi-sensory feedback-a review. In: Jimenez A, M Al Hadithi B, eds. Robot Manipulators Trends and Development. Croatia: InTech, 2010. 587–619
9 Senoo T, Yamakawa Y, Mizusawa S, et al. Skillful manipulation based on high-speed sensorymotor fusion. In: Proceedings of the IEEE International Conference on Robotics and Automation (ICRA), Anchorage, 2009. 1611–1612
10 Li Z, Hsu P, Sastry S. Grasping and coordinated manipulation by a multifingered robot hand. Intl J Robot Res, 1989, 8: 33–50
11 Furukawa N, Namiki A, Taku S, et al. Dynamic regrasping using a high-speed multifingered hand and a high-speed vision system. In: Proceedings of the IEEE International Conference on Robotics and Automation (ICRA), Orlando, 2006. 181–187
12 Garcia-Rodriguez R, Parra-Vega V. Rolling a dynamic object with a planar soft-fingertip robot arm. In: Proceedings of the IEEE International Conference on Intelligent Robots and Systems (IROS), Tokyo, 2013. 2472–2478
13 Peters J, Muelling K, Kober J, et al. Robot skill learning. In: Proceedings of European Conference on AI (ECAI), Montpellier, 2012. 40–45
14 Argall B D, Chernova s, Veloso M, et al. A survey of robot learning from demonstration. Robot Auton Syst, 2009, 57: 469–483
15 Schaedle S, Ertel E. Dexterous manipulation using hierarchical reinforcement learning. In: Proceedings of the IEEE International Conference on Robotics and Automation Workshop, Karlsruhe, 2013. 1–5
16 Kalakrishnan M, Righetti L, Pastor P, et al. Learning force control policies for compliant manipulation. In: Proceedings of the IEEE International Conference on Intelligent Robots and Systems (IROS), San Francisco, 2011. 4639–4644
17 Baier-Lowenstein T, Zhang J. Learning to grasp everyday objects using reinforcement-learning with automatic value cut-off. In: Proceedings of the IEEE International Conference on Intelligent Robots and Systems (IROS), San Diego, 2007. 1551–1556
18 Pelossof R, Miller A, Allen P. An svm learning approach to robotic grasping. In: Proceedings of the IEEE International Conference on Robotics and Automation (ICRA), Barcelona, 2004. 3512–3518
19 Gorce P, Rezzoug N. A method to learn hand grasping posture from noisy sensing information. Robotica, 2004, 22: 309–318
20 Kroemer O, Detry P, Piater J, et al. Combining active learning and reactive control for robot grasping. Robot Auton Syst, 2010, 58: 1105–1116
21 Robles-De-La-Torre G, Hayward V. Force can overcome object geometry in the perception of shape through active touch. Nature, 2001, 412: 445–448
22 Roberts K S. Robot active touch exploration: constraints and strategies. In: Proceedings of the IEEE International Conference on Robotics and Automation (ICRA), Tsukuba, 1990. 980–985
23 Allen P K, Michelman P. Acquisition and interpretation of 3-d sensor data from touch. IEEE Trans Robot Automat, 1990, 6: 397–404
24 Lederman S J, Klatzky R L, Hamilton C L, et al. Perceiving roughness via a rigid probe: psychophysical effects of exploration speed and mode of touch. Electron J Haptics Res, 1999, 1
25 Yoshioka T, Bensmaia S, Craig J, et al. Texture perception through direct and indirect touch: an analysis of perceptual space for tactile textures in two modes of exploration. Somatosens Motor Res, 2007, 24: 53–70
26 Lynch K M. The mechanics of fine manipulation by pushing. In: Proceedings of the IEEE International Conference on Robotics and Automation (ICRA), Ottawa, 1992. 2269–2276

27 Namiki A, Imai Y, Ishikawa M, et al. Development of a high-speed multifingered hand system and its application to catching. In: Proceedings of the IEEE International Conference on Intelligent Robots and Systems (IROS), Nevada, 2003. 2666–2671
28 Flash T. The control of hand equilibrium trajectories in multi-joint arm movements. Biol Cybern, 1987, 57: 257–274
29 Hogan N. The mechanics of multi-joint posture and movement control. Biol Cybern, 1985, 52: 315–331
30 Asada H, Slotine J-J E. Robot Analysis and Control. New York: Wiley, 1986
31 Kim B, Park J, Park S, et al. Impedance learning for robotic contact tasks using natural actor-critic algorithm. IEEE Trans Syst Man Cybern Part B-Cybern, 2010, 40: 433–443
32 Lipkin H, Patterson T. Generalized center of compliance and stiffness. In: Proceedings of the IEEE International Conference on Intelligent Robots and Systems (IROS), Raleigh, 1992. 1251–1256
33 Inoue T, Hirai S. Elastic model of deformable fingertip for softfingered manipulation. IEEE Trans Robot, 2006, 22: 1273–1279